complexes with imidazolate bridges.

(ii) The coordination structure around cobalt in either **3** or **4** approaches that proposed for the Co(III) complex of pseudotetrapeptide A of BLM.[46] Successful structure determination of **3** and **4** now clearly indicates the possibility of coordination of the pyrimidine, β-aminoalanine, and β-hydroxyhistidine moieties of BLM to cobalt in Co^{III}–BLM.

(iii) The identity of the sixth ligand that binds cobalt in orange Co^{III}–BLM has not been established. The present work strongly suggests that characterization of a series of complexes of the composition $[Co(PMA)L]^{n+}$ in which L denotes various ligands that represent other donor functions of BLM could eventually reveal the architecture of the coordination sphere of cobalt in orange Co^{III}–BLM.

Acknowledgment. Financial support from the donors of the Petroleum Research Fund, administered by the American Chemical Society, and a grant from the Cancer Research Coordination Committee of UC is gratefully acknowledged. We thank Jim Loo for help in the COSY experiments.

Supplementary Material Available: SPACFIL drawings of the cations in **3** and **4** (Figures S1 and S2), atomic coordinates and isotropic thermal parameters for the non-hydrogen atoms in **3** (Table S1) and **4** (Table S2), complete lists of bond lengths and angles for **3** (Tables S3 and S4) and **4** (Tables S7 and S8), anisotropic thermal parameters for **3** (Table S5) and **4** (Table S9), and H atom coordinates and isotropic thermal parameters for **3** (Table S6) and **4** (Table S10) (18 pages); values of $10|F_o|$ and $10|F_c|$ (Tables S11 and S12) (35 pages). Ordering information is given on any current masthead page.

Contribution from the Department of Chemistry, Massachusetts Institute of Technology, Cambridge, Massachusetts 02139, and Department of Radiology, Harvard Medical School and Brigham and Women's Hospital, Boston, Massachusetts 02115

Technetium Thiolate Complexes as Oxygen Atom Transfer Catalysts

Nadine de Vries,[1a] Alun G. Jones,[1b] and Alan Davison*,[1a]

Received February 16, 1989

Both Tc(III) compounds $Tc(tmbt)_3(MeCN)_2$ (**6**) and $Tc(tmbt)_3(py)_2$ (**7**) can be oxidized to Tc(V) oxo species by oxygen atom transfer. The initial product of the reaction of **6** with DMSO was characterized by X-ray crystallography and found to be $Tc(tmbt)_3(DMSO)(MeCN)$, the product of ligand substitution, not oxygen atom transfer (crystal data: monoclinic, a = 14.026 (2) Å, b = 26.856 (7) Å, c = 20.025 (3) Å, β = 104.20 (1)°, space group = $P2_1/n$, Z = 8; final R = 0.083, R_w = 0.105). However, compound **6** is oxidized to $TcO(tmbt)_3(py)$ (**1**) by pyridine *N*-oxide, and **7** reacts with a number of other oxygen atom transfer reagents as well to produce the oxotechnetium(V) complex **1**. The Tc(V) oxo compound $TcO(SC_{15}H_{23})_3(NC_5H_5)$ (**1**) was also characterized by X-ray crystallography (crystal data: monoclinic, a = 13.487 (2) Å, b = 17.654 (3) Å, c = 21.603 Å, β = 96.676 (9)°, space group = $P2_1/n$, Z = 4; final R = 0.051, R_w = 0.064). Addition of excess thiolate to **1** yields $(Ph_4As)[TcO(tmbt)_4]$ (**3**), which can also be prepared directly from $(Ph_4As)[TcOCl_4]$. Both **1** and **3** can be reduced by oxygen atom abstraction to restore the Tc(III) tris(thiolate) core. Reaction of **3** with PEt_3 requires much more vigorous conditions than **1** does, but both materials are reduced to $Tc(tmbt)_3(PEt_3)_2$. The oxidative and reductive oxo-transfer reactions can be coupled to complete a catalytic cycle. In the oxidation of PPh_3 by DMSO, the catalyst is still fully active after 500 turnovers.

Oxygen atom transfer reactions of molybdenum have been extensively investigated because molybdoenzymes have been shown to catalyze reactions in which oxygen atoms are added or removed from substrates.[2] In contrast, the analogous chemistry of its neighbor, technetium, is essentially unexplored. Rare examples of such reactions include the removal of the oxo groups from both $TcOCl_2(HB(pz)_3)$[3] and $[TcO(MoS_4)_2]^{-}$[4] by phosphines, and Lu and Clarke have shown pyridine to act as an oxygen atom abstraction agent during the formation of μ-oxo dimers.[5]

Oxotechnetium complexes form a large part of the body of known technetium chemistry, mostly due to their use as diagnostic radiopharmaceutical agents,[6] and a significant number of these contain sulfur ligands.[7-10] We have recently reported the preparation of oxotechnetium(V) anions[11] as well as a series of Tc(III) compounds[12] that incorporate the sterically hindered ligands 2,3,5,6-tetramethylbenzenethiolate (tmbt) and 2,4,6-triisopropylbenzenethiolate (tibt). Conversion of one class of thiolate compound to the other formally involves the addition or removal of an oxygen atom and a concurrent change in the oxidation state of the metal of ±2. We have, therefore, studied the reactions of Tc(III) compounds with oxygen atom donor reagents and those of oxotechnetium(V) species with trialkyl- and triarylphosphines. These reactions and their application to catalysis are discussed herein.

Experimental Section

Caution! Technetium-99 is a weak β^--emitter (E = 0.292 MeV, $t_{1/2}$ = 2.12 × 10^5 years). All work has been done in laboratories approved for the use of low levels of radioactive materials. Precautions have been detailed elsewhere.[7]

Abbreviations used: Htmbt, 2,3,5,6-tetramethylbenzenethiol; Htibt, 2,4,6-triisopropylbenzenethiol.

Ammonium pertechnetate was supplied as a gift by Du Pont/Biomedical Products. The Tc(IV) complex, $(NH_4)_2[TcCl_6]$, was prepared by the method of Nelson et al.,[13] and $(Ph_4As)[TcOCl_4]$ and $(n\text{-}Bu_4N)[TcOCl_4]$ were synthesized by the methods of Trop.[14] Reagents

(1) (a) Massachusetts Institute of Technology. (b) Harvard Medical School.
(2) Holm, R. H. *Chem. Rev.* **1987**, *87*, 1401.
(3) Abrams, M. J.; Davison, A.; Jones, A. G. *Inorg. Chim. Acta* **1984**, *82*, 125.
(4) DuPreez, J. G. H.; Gerber, T. I. A. *Inorg. Chim. Acta* **1985**, *110*, 59.
(5) Lu, J.; Clarke, M. J. *Inorg. Chem.* **1988**, *27*, 4761.
(6) Davison, A.; Jones, A. G. *Int. J. Appl. Radiat. Isot.* **1982**, *33*, 875.
(7) Davison, A.; Orvig, C.; Trop, H. S.; Sohn, M.; DePamphilis, B. V.; Jones, A. G. *Inorg. Chem.* **1980**, *19*, 1988.
(8) Byrne, E. F.; Smith, J. E. *Inorg. Chem.* **1979**, *18*, 1832.
(9) DePamphilis, B. V.; Jones, A. G.; Davison, A. *Inorg. Chem.* **1983**, *22*, 2292.
(10) Spies, H.; Johannsen, B. *Inorg. Chim. Acta* **1981**, *48*, 225.
(11) Davison, A.; de Vries, N.; Dewan, J.; Jones, A. G. *Inorg. Chim. Acta* **1986**, *120*, L15.
(12) de Vries, N.; Dewan, J. C.; Jones, A. G.; Davison, A. *Inorg. Chem.* **1988**, *27*, 1574.
(13) Nelson, C. M.; Boyd, G. E.; Smith, W. T., Jr. *J. Am. Chem. Soc.* **1954**, *76*, 348.

0020-1669/89/1328-3728$01.50/0

and solvents were used as received unless otherwise indicated. The thiol ligands, Htmbt and Htibt, were supplied by Michelle Millar.[15] ^1H and ^{31}P NMR spectra were recorded on a Varian XL-300 spectrometer. Infrared spectra were obtained on an IBM System 9000 FTIR spectrometer, and UV–visible spectra, on an HP 8451A diode array spectrophotometer. Fast atom bombardment mass spectra (FABMS) of samples dissolved in a 3-nitrobenzyl alcohol matrix were recorded with a MAT 731 mass spectrometer equipped with an Ion Tech B11N FAB gun and operating at an accelerating voltage of 8 kV. The FAB gun produced a beam of 6–8-keV xenon neutrals. Elemental analyses were performed by Atlantic Microlab, Norcross, GA. Electrochemical measurements were performed on acetonitrile solutions 0.40 mM in analyte and 0.1 M in $(n\text{-}Bu_4N)ClO_4$ by using a PAR Model 174 polarographic analyzer equipped with a rotating Pt working electrode and a Pt-wire counter electrode. Voltages were measured versus a saturated calomel electrode (SCE).

Syntheses. TcO(tmbt)$_3$(py) (1). Pyridine (5 mL) and three drops of distilled water were added to a solution of $(n\text{-}Bu_4N)[TcOCl_4]$ (221 mg, 0.442 mmol) in 20 mL of MeOH. This mixture was allowed to stir for 10 min until the color was a golden yellow before adding Htmbt (300 mg, 4 equiv) dissolved in MeOH (10 mL). The solution darkened, and overnight an orange solid precipitated. The precipitate was collected, washed with methanol, and dried in vacuo. Recrystallization from CH_2Cl_2/EtOH yielded 292 mg (96%) of dark orange crystalline material.

Anal. Calcd for $C_{35}H_{44}NOS_3Tc$: C, 60.94; H, 6.43; N, 2.03; S, 13.94. Found: C, 60.59; H, 6.46; N, 1.93; S, 13.93. IR (KBr): ν(TcO) 934 cm^{-1}. UV–visible spectrum (CH_2Cl_2): λ_{max} 260 nm (ϵ 44 000 L mol^{-1} cm^{-1}), 290 (47 000), 410 (8500). ^1H NMR (CD_2Cl_2): δ 1.81–2.41 (m, 36 H, ArCH_3), 6.51 (s, 1 H, Ar H), 6.91 (s, 1 H, Ar H), 7.03 (m, 3 H, Ar H and py β-H), 7.53 (t, 1 H, py γ-H), 8.09 (d, 2 H, py α-H). FABMS(+): m/z 1220 (Tc_2O_2(tmbt)$_6^+$), 1055 (Tc_2O_2(tmbt)$_5^+$), 937 (Tc_2(tmbt)$_4$(py)$^+$), 890 (Tc_2O_2(tmbt)$_4^+$), 690 (TcO(tmbt)$_3$(py)H$^+$), 610 (TcO(tmbt)$_3^+$), 524 (TcO(tmbt)$_2$(py)$^+$), 445 (TcO(tmbt)$_2^+$). $E_{1/2}$ (MeCN): +1.35 (irr), −0.82 V (irr).

TcO(tibt)$_3$(py) (2). This compound was prepared analogously to **1**. Yield: 94% as red-orange crystals.

Anal. Calcd for $C_{50}H_{74}NOS_3Tc$: C, 66.71; H, 8.29; N, 1.56; S, 10.68. Found: C, 66.97; H, 8.46; N, 1.68; S, 10.53. IR (KBr): ν(TcO) 914 cm^{-1}. UV–visible spectrum (CH_2Cl_2): λ_{max} 302 nm (ϵ 45 000 L mol^{-1} cm^{-1}), 470 (3000), 708 (300). ^1H NMR ($CDCl_3$): δ 0.57 (d, 6 H, ArCH(CH_3)$_2$), 0.86 (d, 12 H, ArCH(CH_3)$_2$), 0.96 (d, 6 H, ArCH(CH_3)$_2$), 1.00–1.35 (m, 30 H, ArCH(CH_3)$_2$), 2.63 (m, 1 H, ArCH(CH$_3$)$_2$), 2.78 (m, 3 H, ArCH(CH$_3$)$_2$), 2.89 (m, 1 H, ArCH(CH$_3$)$_2$), 3.24 (m, 3 H, ArCH(CH$_3$)$_2$), 3.86 (m, 1 H, ArCH(CH$_3$)$_2$), 6.43 (s, 1 H, Ar H), 6.53 (s, 1 H, Ar H), 6.87 (s, 1 H, Ar H), 6.89 (s, 1 H, Ar H), 6.99 (t, 2 H, py β-H), 7.02 (s, 1 H, Ar H), 7.08 (s, 1 H, Ar H), 7.46 (t, 1 H, py γ-H), 8.28 (d, 2 H, py α-H). FABMS(+): m/z 875 (Tc_2O_3(tibt)$_2$(py)$_2$H$^+$), 820 (TcO(tibt)$_3^+$), 664 (TcO(tibt)$_2^+$).

(Ph$_4$As)[TcO(tmbt)$_4$] (3). The complex $(Ph_4As)[TcOCl_4]$ (113 mg, 0.18 mmol) was dissolved in minimal MeOH, and this solution was added dropwise to a rapidly stirring solution of Htmbt (180 mg, 1.1 mmol) and NaOMe (60 mg, 1.1 mmol) in 10 mL of 1:1 CH_2Cl_2/MeOH. CH_2Cl_2 was removed from the resulting deep red solution under reduced pressure, and a microcrystalline product was collected on a fritted disk, washed with cold methanol, and dried in vacuo. Recrystallization from CH_2Cl_2/hexane produced analytically pure, red crystals. Yield: 150 mg (72%).

Anal. Calcd for $C_{64}H_{72}AsOS_4Tc$: C, 66.25; H, 6.25; S, 11.05. Found: C, 64.50;[16] H, 6.31; S, 10.93. IR (KBr): ν(TcO) 933 cm^{-1}. UV–visible spectrum (CH_2Cl_2): λ_{max} 282 nm (ϵ 56 000 L mol^{-1} cm^{-1}), 440 (7600), 530 (2700). ^1H NMR (CD_2Cl_2): δ 2.07 (s, 12 H, ArCH_3), 2.15 (s, 24 H, ArCH_3), 2.33 (s, 12 H, ArCH_3), 6.74 (s, 4 H, Ar H), 7.58 (d, 8 H, Ph$_4$As α-H), 7.73 (t, 8 H, Ph$_4$As β-H), 7.87 (t, 4 H, Ph$_4$As γ-H). FABMS(+) (of n-Bu$_4$N salt):[17] m/z 1260 (TcO(tmbt)$_4$(n-Bu$_4$N)$_2$), 1221 (Tc_2O_2(tmbt)$_6$H$^+$), 1094 (TcO(tmbt)$_3$(n-Bu$_4$N)$_2^+$), 1055 (Tc_2O_2(tmbt)$_5^+$), 890 (Tc_2O_2(tmbt)$_4^+$), 610 (TcO(tmbt)$_3^+$), 445 (TcO(tmbt)$_2^+$), 330 ((tmbt)$_2^+$). $E_{1/2}$ (MeCN): +0.53 (irr), −0.60 V (irr).

(Ph$_4$As)[TcO(tibt)$_4$] (4). This compound was prepared analogously to **3**. Yield: 77% as red-black microcrystalline material.

Anal. Calcd for $C_{84}H_{112}AsOS_4Tc$: C, 70.07; H, 7.84; S, 8.91. Found: C, 70.14; H, 7.95; S, 8.71. IR (KBr): ν(TcO) 935 cm^{-1}. UV–visible spectrum (CH_2Cl_2): λ_{max} 280 nm (ϵ 57 000 L mol^{-1} cm^{-1}), 334 (17 000), 452 (7600), 554 (3400). ^1H NMR ($CDCl_3$): δ 0.89 (d, 12 H, ArCH(CH_3)$_2$), 0.98 (m, 24 H, ArCH(CH_3)$_2$), 1.20 (d, 24 H, ArCH(CH_3)$_2$), 1.33 (d, 12 H, ArCH(CH_3)$_2$), 2.82 (m, 4 H, ArCH(CH$_3$)$_2$), 3.36 (m, 4 H, ArCH(CH$_3$)$_2$), 4.21 (m, 4 H, ArCH(CH$_3$)$_2$), 6.85 (s, 4 H, Ar H), 6.88 (s, 4 H, Ar H), 7.57 (d, 8 H, Ph$_4$As α-H), 7.73 (t, 8 H, Ph$_4$As β-H), 7.85 (t, 4 H, Ph$_4$As γ-H). FABMS(+) (of n-Bu$_4$N salt):[17] m/z 1056 ((TcO(tibt)$_4$ + H)$^+$), 1040 (Tc(tibt)$_4$H$^+$), 998 ((Tc(tibt)$_4$H − i-Pr)$^+$), 984 ((Tc(tibt)$_4$H$_2$ − i-Pr − Me)$^+$), 956 ((Tc(tibt)$_4$H$_3$ − 2(i-Pr))$^+$), 940 ((Tc(tibt)$_4$H$_2$ − 2(i-Pr) − Me)$^+$), 820 (TcO(tibt)$_3^+$), 802 ((Tc(tibt)$_3$ − 2H)$^+$).

Tc(tmbt)$_3$(PEt$_3$)$_2$ (5). The following was performed under an atmosphere of dinitrogen with use of deoxygenated solvents. Triethylphosphine (500 μL) was added to a solution of Htmbt (500 mg) and NaOMe (200 mg) in methanol (25 mL). This mixture was added via cannula to a second flask containing $(NH_4)_2[TcCl_6]$ (250 mg, 88 mmol). The reaction mixture was allowed to stir at room temperature for 3 h. A blue powder precipitated, which was collected and dried in vacuo. The product was then redissolved in $CHCl_3$ (25 mL) containing PEt_3 (50 μL), and MeOH (25 mL) was added. The chloroform was slowly removed under reduced pressure and the blue precipitate collected, washed with MeOH, and dried in vacuo. Yield: 433 mg of air-sensitive, blue solid (72%).

Anal. Calcd for $C_{42}H_{54}P_2S_3Tc$: C, 60.70; H, 8.37; S, 11.57. Found: C, 60.72; H, 8.29; S, 11.39. UV–visible spectrum (CH_2Cl_2): λ_{max} 326 nm (ϵ 46 000 L mol^{-1} cm^{-1}), 646 (400). ^1H NMR ($CDCl_3$): δ 0.22 (m, 4 H, P(CH_2CH$_3$)$_3$), 0.63 (m, 4 H, P(CH_2CH$_3$)$_3$), 0.89 (m, 4 H, P(CH_2CH$_3$)$_3$), 1.02 (t, 3 H, P(CH$_2$CH_3)$_3$), 1.08 (t, 3 H, P(CH$_2$CH_3)$_3$), 1.47 (m, 12 H, P(CH$_2$CH_3)$_3$), 2.27 (m, 36 H, ArCH_3), 6.89 (s, 2 H, Ar H), 6.95 (s, 1 H, Ar H). FABMS(+): m/z 828 ((Tc(tmbt)$_3$(PEt$_3$)$_2$ − H$_2$)$^+$), 800 ((Tc(tmbt)$_3$(PEt$_3$)$_2$ − Et − H)$^+$), 726 (TcO(tmbt)$_3$(PEt$_3$)H$_2^+$), 710 ((Tc(tmbt)$_3$(PEt$_3$) − 2H)$^+$), 663 ((Tc(tmbt)$_2$(PEt$_3$)$_2$ − 2H)$^+$).

Tc(tmbt)$_3$(py)$_2$ (7). Method 1. Tc(tmbt)$_3$(MeCN)$_2$ (**6**)[12] (63 mg, 0.093 mmol) was placed in MeOH (25 mL) to which 1 mL of pyridine had been added. The mixture was set to reflux for 4 h under an atmosphere of dinitrogen and cooled to room temperature. The microcrystalline green solid that precipitated was collected on a fritted disk, washed with methanol, and dried in vacuo. It was recrystallized by adding methanol to a methylene chloride solution of the product. Yield: 56 mg (82%) of bright green microcrystalline material.

Method 2. The following reaction was performed under an atmosphere of dinitrogen with use of only freshly distilled solvents. Pyridine (2.5 mL) in MeOH (15 mL) was added via cannula to a flask containing $(NH_4)_2[TcCl_6]$ (110 mg, 0.32 mmol), Htmbt (170 mg, 1.03 mmol), Zn dust (100 mg), and MeCN (15 mL). The resulting dark purple mixture was stirred at room temperature for 2 h, opened to the air, and filtered to separate a green precipitate, which was recrystallized by adding methanol to a methylene chloride solution of the product, collected on a fritted disk, and dried in vacuo. Yield: 183 mg (78%) of bright green microcrystalline material.

Anal. Calcd for $C_{40}H_{49}N_2S_3Tc$: C, 63.81; H, 6.56; N, 3.72; S, 12.77. Found: C, 62.84; H, 6.52; N, 3.76; S, 12.78. UV–visible spectrum (CH_2Cl_2): λ_{max} 324 nm (ϵ 40 000 L cm^{-1} mol^{-1}), 428 (5000), 716 (500). ^1H NMR ($CDCl_3$): δ 1.7–2.4 (m, 36 H, ArCH_3), 5.92 (t, 2 H, py β-H), 6.54 (s, 2 H, Ar H), 6.50 (m, 4 H, py β-H, py γ-H, and Ar H), 7.03 (t, 1 H, py γ-H), 7.74 (d, 2 H, py α-H), 8.52 (d, 2 H, py α-H). FABMS-(+): m/z 752 (Tc(tmbt)$_3$(py)$_2^+$), 673 ((Tc(tmbt)$_3$(py)$^+$), 593 ((Tc-(tmbt)$_3$ − H)$^+$), 428 ((Tc(tmbt)$_2$ − H)$^+$).

Tc(tibt)$_3$(py)$_2$ (8). This compound can be prepared by either of the two methods described above for **7**: method 1, yield 80% as bright green microcrystalline material; method 2, yield 74% as bright green microcrystalline material.

Anal. Calcd for $C_{55}H_{79}N_2S_3Tc$: C, 68.57; H, 8.27; N, 2.91; S, 9.98. Found: C, 68.04;[16] H, 8.46; N, 2.96; S, 10.07. UV–visible spectrum (CH_2Cl_2): λ_{max} 328 nm (ϵ 41 000 L cm^{-1} mol^{-1}), 426 (12 000), 658 (800), 734 (1000). ^1H NMR ($CDCl_3$): δ 0.8–1.3 (m, 54 H, ArCH(CH_3)$_2$), 5.91 (br, 2 H, py β-H), 6.22 (s, 2 H, Ar H), 6.50 (t, 1 H, py γ-H), 6.6 (m, 4 H, Ar H, py β-H, and py γ-H), 7.03 (br, 2 H, py α-H), 8.72 (d, 2 H, α-py). FABMS(+): m/z 963 (Tc(tibt)$_3$(py)$_2$H$^+$), 884 (Tc-(tibt)$_3$(py)H$^+$), 820 (TcO(tibt)$_3^+$), 803 ((Tc(tibt)$_3$ − H)$^+$), 789 ((Tc-(tibt)$_3$ − Me)$^+$).

Reactions. Reaction of 3 with PEt$_3$. The following was performed under an atmosphere of dinitrogen with use of deoxygenated solvents. Compound **3** (77 mg, 0.066 mmol) was dissolved in neat PEt_3 (5 mL), and the solution was refluxed for 3 h. Most of the phosphine was removed in vacuo, and the resulting blue oil was dissolved in 50 mL of 1:1

(14) Trop, H. S. Ph.D. Thesis, Massachusetts Institute of Technology, 1979.
(15) Department of Chemistry, SUNY Stony Brook. Thiols were prepared according to: Blower, P. J.; Dilworth, J. R.; Hutchinson, J. P.; Zubieta, J. A. *J. Chem. Soc., Dalton Trans.* **1985**, 1533.
(16) Workers in our laboratories have often noticed that, although samples analyze extremely well for other elements, carbon analyses can be up to one carbon low. A possible explanation is that incomplete combustion, resulting in the formation of TcC, leads to erroneous results.
(17) The n-Bu$_4$N derivative was prepared similarly to the Ph$_4$As salt by using $(n\text{-}Bu_4N)[TcOCl_4]$ as the starting material.

Table I. X-ray Data for the Structure Determination of **2**

$C_{50}H_{74}NOS_3Tc$	space group = $P2_1/n$
fw = 898.32	T = 22 °C
a = 13.487 (2) Å	λ = 0.710 69 Å, graphite monochromated
b = 17.654 (3) Å	ρ_{calcd} = 1.17 g/cm^3, ρ_{exp} = 1.15 g/cm^3
c = 21.603 (2) Å	μ = 4.25 cm^{-1}
β = 96.676 (9)°	transm coeff = 1.33–0.85
V = 5143.7 (8) Å^3	R = 0.051
Z = 4	R_w = 0.064

glacial acetic acid/hexane. The addition of water (2 mL) caused the organic and aqueous layers to separate. The hexane layer was collected and washed thoroughly with water (3 × 15 mL), and the solvent was removed in vacuo. The product was redissolved in CH_2Cl_2 (5 mL), MeOH (5 mL) was added, and CH_2Cl_2 was removed under reduced pressure to produce a blue solid that was spectroscopically identical with **5**. Yield: 23 mg (40%).

Reaction of 1 with PEt_3. Compound **1** (41 mg, 0.060 mmol) was placed in deoxygenated CH_2Cl_2 (15 mL) and the solution placed under an atmosphere of dinitrogen. A stoichiometric amount of PEt_3 (29 μL, 3 equiv) was added via syringe, and the reaction mixture was allowed to stir at ambient temperature for 1 h, at which point the color of the solution had changed from red to bright blue. MeOH (10 mL) was added via cannula, and most of the solvent was removed in vacuo. An air-sensitive blue solid formed, which was collected, washed with MeOH, and dried in vacuo. This compound is spectroscopically identical with **5**. Yield: 19 mg (59%).

Reaction of $Tc(tmbt)_3(MeCN)_2$ (6) with DMSO. 1. Compound **6** (42 mg) and DMSO (5 mL) were placed in a vial that was sealed with a septum, and this mixture was heated to 90 °C for 15 min. Methanol (5 mL) was then introduced via syringe, and the purple solution was allowed to cool. Both the purple product, $Tc(tmbt)_3(MeCN)(DMSO)$ (**9**), and some unreacted starting material crystallized from the solution. The solid was collected on a fritted disk, washed with cold methanol, and dried in vacuo. The instability of the product in solution precluded any attempts at purification.

FABMS(+): m/z 714 (M^+), 673 ((MH − MeCN)$^+$), 636 ((MH − DMSO)$^+$), 610 ($TcO(tmbt)_3^+$), 594 ($Tc(tmbt)_3^+$).

2. If, instead of adding methanol to the above solution, it is allowed to reflux for 1 h, an orange solution results that yields no stable products.

Reaction of 6 with Triethylamine *N*-Oxide. Compound **6** (46 mg, 0.068 mmol) and triethylamine *N*-oxide (21 mg, 3 equiv) were placed in EtOH (20 mL), and the mixture was allowed to reflux for 25 min. At this point, the color of the solution had changed from blue to red-orange, but no stable products could be isolated from the reaction mixture.

Reaction of 6 with Pyridine *N*-Oxide. Compound **6** (24 mg, 0.035 mmol), pyridine *N*-oxide (7.0 mg), and EtOH (20 mL) were combined and refluxed for 10 min. When the solution was cooled, an orange precipitate formed, which was collected on a fritted disk, washed with cold EtOH, and dried in vacuo. This material is spectroscopically identical with **1**. Yield: 6.3 mg (30%).

Reaction of $Tc(tmbt)_3(py)_2$ (7) with Pyridine *N*-Oxide. Compound **7** (32.1 mg, 0.043 mmol), pyridine *N*-oxide (10.2 mg), and EtOH (20 mL) were combined and refluxed for 10 min. When the solution was cooled, an orange precipitate formed, which was collected on a fritted disk, washed with cold EtOH, and dried in vacuo. This material is spectroscopically identical with **1**. Yield: 10.4 mg (36%).

Reaction of 7 with Triethylamine *N*-Oxide. Compound **7** (42.9 mg, 0.057 mmol), triethylamine *N*-oxide (13.8 mg), and EtOH (20 mL) were combined and refluxed for 10 min. When the solution was cooled, an orange precipitate formed, which was collected on a fritted disk, washed with cold EtOH, and dried in vacuo. This material is spectroscopically identical with **1**. Yield: 15.0 mg (38%).

Reaction of 7 with DMSO. Compound **7** (51.2 mg, 0.068 mmol), DMSO (25.0 μL), and EtOH (20 mL) were combined and refluxed for 10 min. When the solution was cooled, an orange precipitate formed, which was collected on a fritted disk, washed with cold EtOH, and dried in vacuo. This material is spectroscopically identical with **1**. Yield: 15.0 mg (32%).

Catalytic Oxidation of PPh_3 by DMSO. Triphenylphosphine (49 mg, 0.187 mmol) and DMSO (15 μL, 0.195 mmol) were placed in deoxygenated MeCN (30 mL). A catalytic amount of compound **1** (1.21 mg, 1.73 μmol) was added and the reaction mixture heated to 45 °C for 3 h. The Me_2S that was produced was removed from solution with a stream of dinitrogen, which was then passed through an aqueous solution of $HgCl_2$. The $(Me_2S)_2{\cdot}3HgCl_2$ that precipitated was collected, dried, identified by its melting point,[18] and quantitated. The conversion of DMSO to Me_2S was 91%. Alternatively, the reaction was monitored by ^{31}P NMR spectroscopy. Plotting the conversion of PPh_3 to $OPPh_3$ versus time showed the rate of catalysis to be 3.9 × 10^{-2} turnover/min for **1** (Figure 5), 9.8 × 10^{-3} turnover/min for **3**, and 0.27 turnover/min for $TcO(SPh)_3(py)$[19] at 22 °C in MeCN.

(18) Szmant, H. H.; Cox, O. *J. Org. Chem.* **1966**, *31*, 1595.

Table II. Non-Hydrogen Atomic Positional Parameters for **2**

atom	x	y	z
Tc1	0.42519 (3)	0.05454 (2)	0.12991 (2)
S1	0.57140 (9)	0.03962 (7)	0.19328 (6)
S2	0.34450 (8)	−0.00483 (7)	0.20320 (6)
S3	0.3070 (1)	0.14749 (7)	0.13170 (6)
O1	0.4110 (3)	−0.0031 (2)	0.0685 (2)
N1	0.5215 (3)	0.1341 (2)	0.0856 (2)
C11	0.5598 (3)	−0.0024 (3)	0.2670 (2)
C12	0.5684 (4)	−0.0810 (3)	0.2745 (2)
C13	0.5592 (4)	−0.1108 (3)	0.3333 (3)
C14	0.5430 (4)	−0.0658 (3)	0.3836 (2)
C15	0.5371 (4)	0.0108 (3)	0.3744 (3)
C16	0.5459 (3)	0.0449 (3)	0.3178 (2)
C17	0.5875 (5)	−0.1337 (3)	0.2231 (3)
C18	0.5004 (6)	−0.1858 (4)	0.2053 (4)
C19	0.6829 (6)	−0.1803 (4)	0.2409 (4)
C21	0.2130 (3)	0.0123 (3)	0.1929 (2)
C22	0.1721 (3)	0.0561 (3)	0.2378 (2)
C23	0.0686 (4)	0.0654 (3)	0.2308 (3)
C24	0.0071 (4)	0.0332 (3)	0.1816 (3)
C25	0.0503 (4)	−0.0093 (3)	0.1396 (3)
C26	0.1519 (4)	−0.0217 (3)	0.1439 (3)
C27	0.2351 (4)	0.0904 (3)	0.2935 (3)
C28	0.1963 (5)	0.1666 (4)	0.3120 (4)
C29	0.2482 (6)	0.0374 (4)	0.3471 (3)
C31	0.3321 (3)	0.2265 (2)	0.0844 (2)
C32	0.3090 (4)	0.2232 (3)	0.0197 (2)
C33	0.3296 (4)	0.2863 (3)	−0.0145 (2)
C34	0.3705 (5)	0.3515 (3)	0.0123 (3)
C35	0.3872 (5)	0.3533 (3)	0.0761 (3)
C36	0.3697 (4)	0.2928 (3)	0.1135 (3)
C37	0.2594 (5)	0.1544 (3)	−0.0121 (3)
C38	0.2910 (8)	0.1400 (5)	−0.0772 (3)
C39	0.1470 (6)	0.1614 (4)	−0.0143 (4)
C101	0.5698 (4)	0.1920 (3)	0.1149 (3)
C102	0.6283 (5)	0.2408 (4)	0.0863 (4)
C103	0.6397 (5)	0.2295 (4)	0.0259 (4)
C104	0.5929 (6)	0.1702 (4)	−0.0047 (3)
C105	0.5342 (5)	0.1243 (3)	0.0263 (3)
C110	0.5273 (5)	−0.1009 (4)	0.4457 (3)
C111	0.6080 (7)	−0.1556 (6)	0.4688 (4)
C112	0.4259 (7)	−0.1311 (7)	0.4458 (4)
C113	0.5405 (4)	0.1300 (3)	0.3104 (3)
C114	0.4891 (5)	0.1705 (3)	0.3602 (3)
C115	0.6427 (5)	0.1643 (4)	0.3078 (4)
C210	−0.1054 (5)	0.0447 (5)	0.1766 (5)
C211	−0.1342 (7)	0.1203 (7)	0.1579 (6)
C212	−0.1487 (6)	0.015 (1)	0.2293 (7)
C213	0.1921 (4)	−0.0720 (3)	0.0954 (3)
C214	0.1587 (7)	−0.0490 (4)	0.0293 (3)
C215	0.1634 (6)	−0.1537 (4)	0.1043 (3)
C310	0.3932 (7)	0.4197 (4)	−0.0273 (4)
C311	0.3090 (8)	0.4689 (5)	−0.0409 (5)
C312	0.4538 (9)	0.4013 (6)	−0.0772 (5)
C313	0.3850 (6)	0.3004 (3)	0.1842 (3)
C314	0.2857 (8)	0.3222 (5)	0.2072 (4)
C315	0.4671 (8)	0.3549 (5)	0.2081 (4)

Table III. Selected Bond Distances and Angles for **2**

Bond Lengths (Å)			
Tc1–O1	1.665 (3)	Tc1–S2	2.278 (1)
Tc1–N1	2.205 (4)	Tc1–S3	2.291 (1)
Tc1–S1	2.281 (1)		
Bond Angles (deg)			
N1–Tc1–O1	93.6 (2)	S1–Tc1–S2	88.82 (4)
S1–Tc1–O1	114.7 (1)	S2–Tc1–S3	85.89 (4)
S2–Tc1–O1	104.6 (1)	S1–Tc1–S3	128.84 (5)
S3–Tc1–O1	115.8 (1)	C11–S1–Tc1	115.2 (1)
N1–Tc1–S2	161.4 (1)	C21–S2–Tc1	112.5 (2)
N1–Tc1–S1	79.8 (1)	C31–S3–Tc1	111.8 (2)
N1–Tc1–S3	89.8 (1)		

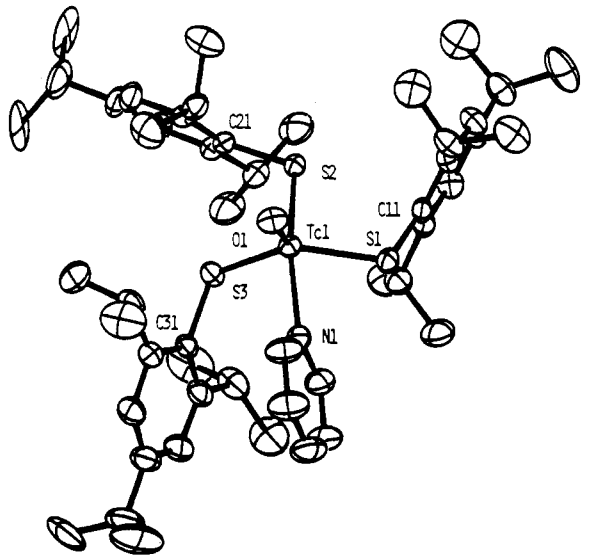

Figure 1. ORTEP diagram of **2** showing the partial atom-labeling scheme and 30% probability ellipsoids.

Table IV. X-ray Data for the Structure Determination of **9**

$C_{34}H_{48}NOS_4Tc$	space group = $P2_1/n$
fw = 713.91	T = 22 °C
a = 14.026 (2) Å	λ = 0.710 69 Å, graphite monochromated
b = 26.856 (7) Å	ρ_{calcd} = 1.29 g/cm^3, ρ_{exp} = 1.31 g/cm^3
c = 20.025 (3) Å	μ = 6.25 cm^{-1}
β = 104.20 (1)°	transm coeff = 1.39–0.50
V = 7543.1 (9) Å^3	R = 0.083
Z = 8	R_w = 0.105

X-ray Crystal Structure Determinations. $TcO(SC_{15}H_{23})_3(NC_5H_5)$. Crystal data are presented in Table I, atomic positional parameters in Table II, and selected bond distances and angles in Table III, and an ORTEP diagram is shown in Figure 1. Red X-ray-quality prismatic crystals were grown by slow evaporation of a methylene chloride/methanol solution of **2**. A crystal having the approximate dimensions of 0.2 × 0.2 × 0.2 mm was chosen, and the space group was determined unambiguously to be $P2_1/n$. A total of 12 686 reflections (of which 12 184 were unique, R_{int} = 0.004) were collected on a Rigaku AFC6R diffractometer (max 2θ = 55.1°; octants collected $+h,+k,\pm l$; scan mode ω–2θ). Solution and refinement of the structure were carried out by using SHELX-76 and the TEXSAN programs of the Molecular Structure Corp. Neutral-atom scattering factors were used throughout,[20] and no extinction effects were observed. The structure was solved by using Patterson methods, an absorption correction was applied by using DIFABS, and all non-hydrogen atoms were refined anisotropically. Hydrogen atoms were refined from their calculated positions. Final residuals are R = 0.051 and R_w = 0.064.[21]

$Tc(SC_{10}H_{13})_3(CH_3CN)((CD_3)_2SO)$. Crystal data are presented in Table IV, atomic positional parameters in Table V, and selected bond lengths and angles in Table VI, and an ORTEP diagram is shown in Figure 2. Purple prisms were grown from a solution of **9** in DMSO-d_6. A monoclinic crystal of approximate dimensions 0.4 × 0.4 × 0.6 mm was chosen, and the space group was determined unambiguously to be $P2_1/n$. A total of 13 845 reflections (of which 13 269 were unique, R_{int} = 0.012) were collected on a Rigaku AFC6R diffractometer (max 2θ = 50.2°; octants collected $+h,+k,\pm l$; scan mode ω–2θ). Solution and refinement of the structure were carried out as described above. Due to the poor quality of the data, only the Tc and S atoms were refined anisotropically and all other atoms were refined isotropically. Hydrogen atoms were ignored. Final residuals are R = 0.083 and R_w = 0.105.[21]

Results and Discussion

Synthesis and Characterization of Compounds. Oxotechnetium(V) Complexes. The room-temperature reaction of $[TcOCl_4]^-$ with excess pyridine (20% in MeOH) to produce the *trans*-dioxo species $[TcO_2(py)_4]^+$ has long been known,[22,23] and the pyridine ligands in this complex have been shown to be labile and easily displaced.[24] Formation of the *trans*-dioxo complex in situ followed by the addition of 2,3,5,6-tetramethylbenzenethiol (Htmbt) causes the slow replacement of three of the pyridines by thiolate ligands, producing $TcO(tmbt)_3(py)$ (**1**) in nearly quantitative yields. This reaction strongly favors the formation of the neutral compound with one pyridine and three thiolate ligands, and compounds of other stoichiometries are not observed. In contrast to the preparation of **1** in the presence of a large excess of pyridine, isolated $[TcO_2(py)_4](PF_6)$ reacts with Htmbt upon the time of mixing to yield the same product. Dependence of the reaction rate upon the concentration of leaving group suggests that the reaction mechanism is dissociative.[25] To ensure that the large excess of pyridine is not slowing the rate by preventing protonation and subsequent loss of one of the oxo groups, a "noncoordinating" proton sponge (1,1,2,2-tetramethylguanidine) was introduced into the reaction of isolated $[TcO_2(py)_4](PF_6)$ with Htmbt in lieu of excess pyridine. The rate was similar to that observed for the reaction of $[TcO_2(py)_4](PF_6)$ and Htmbt alone, suggesting that protonation and loss of the oxo group is not a rate-determining factor.

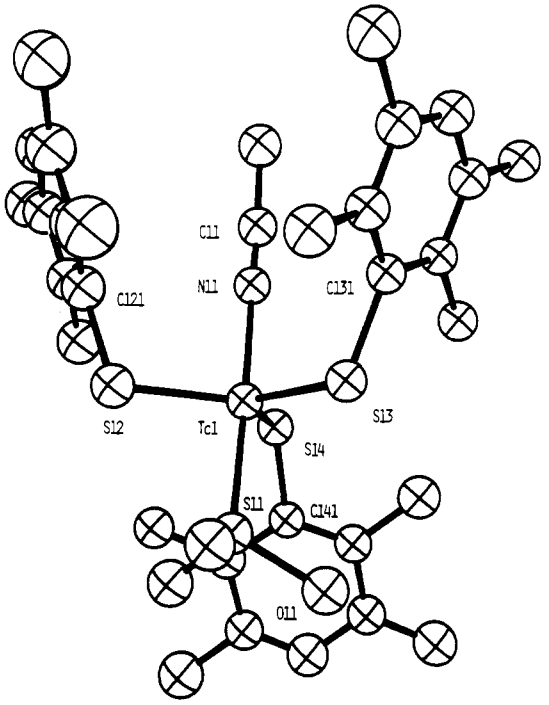

Figure 2. ORTEP diagram of fragment 1 of **9** showing the partial atom-labeling scheme and 30% probability ellipsoids.

The reaction of isolated $TcO(SAr)_3(py)$ with excess thiolate leads to slow substitution of the lone pyridine ligand and yields $[TcO(SAr)_4]^-$. Alternatively, $(Ph_4As)[TcO(SAr)_4]$ can be prepared directly from $(Ph_4As)[TcOCl_4]$. Although this simple ligand-exchange reaction appears straightforward, the desired product is only formed under strictly controlled conditions. A solution of $[TcOCl_4]^-$ must be added slowly to a second solution containing the deprotonated thiol in order to ensure that the thiolate ligand is always in excess, thereby preventing thiolate bridging. Unlike the more kinetically stable oxo complexes with bidentate thiolates (i.e. $[TcO(ethanedithiolato)_2]^-$ [8]), compounds **3** and **4** in alkaline methanolic solutions are slowly oxidized by air to form $[TcO_4]^-$.

(19) $TcO(SPh)_3(py)$ was prepared analogously to **1** and **2** and characterized by IR, FABMS(+), and ^1H NMR methods.
(20) *International Tables for X-Ray Crystallography*; Kynoch: Birmingham, England, 1974; Vol. IV.
(21) Anomalous dispersion effects were included in F_c: Ibers, J. A.; Hamilton, W. C. *Acta Crystallogr.* **1964**, *17*, 781.
(22) Kusina, A. F.; Oblova, A. A.; Spitsyn, V. I. *Zh. Neorg. Khim.* **1972**, *17*, 1377.
(23) Trop, H. S. Ph.D. Thesis, Massachusetts Institute of Technology, 1979; p 64.
(24) Pearlstein, R. M.; Davison, A. Unpublished results.
(25) Langford, C. H.; Gray, H. B. *Ligand Substitution Processes*; W. A. Benjamin, Inc.: London, 1966; Chapter 1.

Table V. Atomic Positional Parameters for **9**

atom	x	y	z	atom	x	y	z
Tc1	0.26704 (7)	0.04700 (4)	0.24205 (5)	C1310	0.381 (1)	−0.0695 (7)	0.3829 (8)
Tc2	0.80430 (6)	0.25203 (4)	0.37701 (4)	C141	0.1197 (9)	0.1147 (5)	0.1107 (6)
S11	0.1538 (2)	0.0900 (1)	0.2844 (2)	C142	0.149 (1)	0.1645 (6)	0.1083 (7)
S12	0.3842 (2)	0.0939 (1)	0.3118 (1)	C143	0.066 (1)	0.1977 (7)	0.0929 (8)
S13	0.2057 (3)	−0.0244 (1)	0.2751 (2)	C144	−0.028 (1)	0.1831 (7)	0.0830 (7)
S14	0.2173 (2)	0.0689 (1)	0.1308 (2)	C145	−0.052 (1)	0.1357 (7)	0.0837 (7)
S21	0.9124 (2)	0.2031 (1)	0.3375 (1)	C146	0.021 (1)	0.0959 (6)	0.0969 (7)
S22	0.6822 (2)	0.2081 (1)	0.3082 (1)	C147	0.253 (1)	0.1810 (7)	0.1195 (8)
S23	0.8528 (2)	0.2336 (1)	0.4894 (1)	C148	0.096 (2)	0.257 (1)	0.096 (1)
S24	0.8769 (2)	0.3185 (1)	0.3410 (2)	C149	−0.158 (1)	0.1178 (7)	0.0714 (8)
O11	0.0481 (6)	0.0798 (3)	0.2570 (4)	C1410	−0.003 (1)	0.0402 (6)	0.0963 (7)
O21	1.0188 (6)	0.2132 (3)	0.3614 (4)	C221	0.5619 (7)	0.2302 (4)	0.3082 (5)
N11	0.3739 (6)	0.0071 (4)	0.2083 (4)	C222	0.5088 (8)	0.2575 (5)	0.2514 (6)
N21	0.7022 (6)	0.2991 (3)	0.4064 (4)	C223	0.4173 (8)	0.2751 (5)	0.2529 (6)
C11	0.4350 (8)	−0.0120 (5)	0.1902 (5)	C224	0.3753 (8)	0.2625 (5)	0.3067 (6)
C12	0.516 (1)	−0.0413 (6)	0.1750 (7)	C225	0.4262 (8)	0.2333 (5)	0.3613 (5)
C13	0.177 (1)	0.0813 (5)	0.3772 (6)	C226	0.5190 (7)	0.2166 (4)	0.3631 (5)
C14	0.1685 (9)	0.1569 (5)	0.2833 (6)	C227	0.5502 (9)	0.2679 (5)	0.1889 (6)
C21	0.6454 (9)	0.3233 (5)	0.4183 (6)	C228	0.360 (1)	0.3108 (6)	0.1961 (7)
C22	0.564 (1)	0.3588 (5)	0.4238 (6)	C229	0.3739 (8)	0.2200 (5)	0.4187 (6)
C23	0.8859 (9)	0.2045 (5)	0.2453 (6)	C2210	0.5762 (8)	0.1834 (5)	0.4213 (5)
C24	0.895 (1)	0.1372 (5)	0.3470 (6)	C231	0.9470 (8)	0.1869 (5)	0.5143 (5)
C121	0.5060 (8)	0.0759 (5)	0.3102 (5)	C232	0.9198 (9)	0.1401 (5)	0.5287 (6)
C122	0.562 (1)	0.0498 (5)	0.3672 (6)	C233	0.994 (1)	0.1005 (6)	0.5490 (6)
C123	0.658 (1)	0.0335 (7)	0.3606 (9)	C234	1.089 (1)	0.1141 (6)	0.5518 (7)
C124	0.689 (1)	0.0450 (6)	0.3054 (8)	C235	1.117 (1)	0.1610 (6)	0.5398 (6)
C125	0.641 (1)	0.0716 (6)	0.2544 (7)	C236	1.0474 (9)	0.2018 (5)	0.5226 (6)
C126	0.5442 (8)	0.0894 (5)	0.2534 (6)	C237	0.809 (1)	0.1262 (6)	0.5199 (7)
C127	0.526 (1)	0.0387 (6)	0.4313 (8)	C238	0.968 (1)	0.0486 (7)	0.5662 (8)
C128	0.716 (2)	0.0006 (9)	0.424 (1)	C239	1.227 (1)	0.1737 (7)	0.5471 (8)
C129	0.684 (1)	0.0851 (7)	0.1933 (9)	C2310	1.074 (1)	0.2557 (5)	0.5122 (6)
C1210	0.485 (1)	0.1207 (6)	0.1961 (6)	C241	0.8203 (9)	0.3756 (5)	0.3560 (6)
C131	0.2767 (8)	−0.0753 (5)	0.2578 (6)	C242	0.746 (1)	0.3953 (6)	0.3040 (7)
C132	0.255 (1)	−0.0972 (5)	0.1927 (6)	C243	0.701 (1)	0.4403 (7)	0.3167 (8)
C133	0.316 (1)	−0.1345 (6)	0.1789 (7)	C244	0.735 (1)	0.4641 (5)	0.3790 (7)
C134	0.398 (1)	−0.1489 (6)	0.2301 (8)	C245	0.809 (1)	0.4448 (6)	0.4262 (7)
C135	0.419 (1)	−0.1278 (6)	0.2927 (7)	C246	0.853 (1)	0.4009 (6)	0.4189 (7)
C136	0.357 (1)	−0.0937 (5)	0.3099 (7)	C247	0.712 (1)	0.3699 (8)	0.2352 (9)
C137	0.171 (1)	−0.0773 (6)	0.1347 (7)	C248	0.613 (1)	0.4613 (7)	0.2580 (9)
C138	0.301 (1)	−0.1581 (7)	0.1072 (8)	C249	0.845 (1)	0.4757 (7)	0.4944 (8)
C139	0.519 (1)	−0.1430 (8)	0.346 (1)	C2410	0.934 (1)	0.3777 (6)	0.4754 (7)

Table VI. Selected Bond Distances and Angles for **9**

	Fragment 1		
	Bond Lengths (Å)		
Tc1–S11	2.289 (3)	Tc1–S14	2.242 (3)
Tc1–S12	2.261 (3)	Tc1–N11	2.085 (8)
Tc1–S13	2.265 (4)	N11–C11	1.13 (1)
	Bond Angles (deg)		
S12–Tc1–N11	90.0 (2)	S12–Tc1–S13	124.2 (1)
S12–Tc1–S11	87.4 (1)	S12–Tc1–S14	118.0 (1)
S13–Tc1–N11	90.8 (3)	S13–Tc1–S14	117.6 (1)
S13–Tc1–S11	88.3 (1)	C121–S12–Tc1	113.1 (4)
S14–Tc1–N11	83.5 (2)	C131–S13–Tc1	108.9 (4)
S14–Tc1–S11	99.3 (1)	C141–S14–Tc1	115.7 (4)
S11–Tc1–N11	177.2 (2)		
	Fragment 2		
	Bond Lengths (Å)		
Tc2–S21	2.289 (3)	Tc2–S24	2.259 (4)
Tc2–S22	2.250 (3)	Tc2–N21	2.099 (9)
Tc2–S23	2.240 (3)	N21–C21	1.10 (1)
	Bond Angles (deg)		
S22–Tc2–N21	91.1 (2)	S22–Tc2–S23	119.8 (1)
S22–Tc2–S21	87.5 (1)	S22–Tc2–S24	123.6 (1)
S23–Tc2–N21	84.9 (2)	S23–Tc2–S24	116.4 (1)
S23–Tc2–S21	99.0 (1)	C221–S22–Tc2	113.7 (4)
S24–Tc2–N21	90.3 (3)	C231–S23–Tc2	117.0 (3)
S24–Tc2–S21	87.4 (1)	C241–S24–Tc2	111.8 (4)
S21–Tc2–N21	176.0 (2)		

Compounds **1**–**4** are diamagnetic and have easily interpretable ^{1}H NMR spectra. Each of the three thiolate rings on **1** and **2** are inequivalent and asymmetric, while the pyridine ligand, which is probably spinning rapidly, appears symmetric, giving rise to only three signals. The tetrathiolate complexes **3** and **4** both show all four thiolate ligands to be magnetically equivalent.

The IR stretching frequencies of the Tc=O group in the tmbt and tibt tetrathiolate complexes **3** and **4** are identical with each other within the limits of detection (934 cm^{-1}) and are typical for Tc(V) oxo complexes with thiolate ligands. In contrast, the Tc=O stretch for compound **2** is found at 914 cm^{-1}, while that of the less sterically hindered complex occurs at 934 cm^{-1}.

The mass spectra of the tmbt compounds **1** and **3** show that some dimer formation occurs in the FAB matrix. This is especially evident for the neutral compound **1** where loss of the pyridine ligand facilitates dimer formation. The addition of a stoichiometric amount of free thiol (Htmbt) to the FAB matrix results in a mass spectrum of **1** that is indistinguishable from that of the tetrathiolate species **3**. The analogous tibt complexes **2** and **4** are too bulky to form dimers, and only monomeric peaks are observed.

Technetium(III) Compounds. The Tc(III) compound Tc(tmbt)$_3$(py)$_2$ (**7**) can be prepared by two methods. The more efficient is ligand exchange from Tc(tmbt)$_3$(MeCN)$_2$ (**6**). Compound **6** and a large excess of pyridine are placed in methanol and set to reflux for 4 h at which point the product **7** precipitates as a bright green microcrystalline material. Alternatively, compound **7** can be prepared directly from $(NH_4)_2[TcCl_6]$. Addition of pyridine to a slurry of $(NH_4)_2[TcCl_6]$, thiol ligand, and zinc dust in deoxygenated methanol leads to a dark magenta solution that deposits the product as a green powder. Thiolate alone is sufficient as the reductant, but zinc has been shown to be an effective reductant in basic methanolic solutions[26] and improves

(26) Hills, A.; Leigh, G. J.; Hutchinson, J.; Zubieta, J. A. *J. Chem. Soc., Dalton Trans* **1985**, 1069.

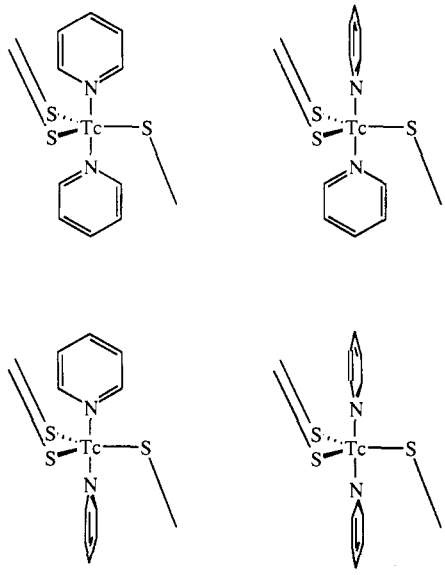

Figure 3. Schematic representation of the possible orientations of the pyridine rings in $Tc(SAr)_3(py)_2$.

the yield. Solutions of **7** are stable to the air and only decompose after a few days.

The bis(phosphine) compound $Tc(tmbt)_3(PEt_3)_2$ (**5**) can also be prepared in good yield from $(NH_4)_2[TcCl_6]$. Phosphines are effective reducing agents, and in contrast to the analogous synthesis of $Tc(tmbt)_3(py)_2$, the addition of zinc has no effect on the yield. Compound **5** is isolated as a bright blue and air-sensitive powder.

Compounds **5** and **7** exhibit many of the properties of the previously reported Tc(III) tris(thiolato) compounds with π-accepting coligands.[12] The ^1H NMR spectra of **5** and **7** show that in each case the non-thiolate ligands are inequivalent and that the arenethiolate rings appear in a 2:1 ratio. X-ray crystallographic studies have consistently shown that compounds of the general formula $Tc^{III}(SAr)_3L_2$ are trigonal bipyramidal. Furthermore, there is always a "two-up–one-down" disposition of the arenethiolate rings (see Figure 2). This conformation of the thiolate ligands is responsible both for the 2:1 integral ratio of the arene rings and for the inequivalence of the axial ligands. Thus, from the ^1H NMR data we can assign the diamagnetic compounds **5** and **7** trigonal-bipyramidal geometries and the ligand conformation described above.

The "two-up–one-down" orientation of the arene rings is locked on the NMR time scale, and thus the axial ligands are magnetically inequivalent. The ^1H NMR spectra of compounds **5** and **7** show that the axial ligands are not only inequivalent but asymmetric as well. The bis(phosphine) complexes show complex patterns for the ethyl groups that can only be explained if it is assumed that the phosphine ligands are not free to rotate about the Tc–P bond. The bis(pyridine) compounds **7** and **8** also have magnetically inequivalent axial ligands, and the ^1H NMR spectra of these compounds show an even more complex situation for the axial ligands. For example, in the room-temperature spectrum of the tmbt compound **7**, only two sets of pyridine signals are observed, one for each ring. This suggests either that there is a plane of symmetry running perpendicular to the pyridine rings or that they are spinning rapidly (Figure 3). The ambient-temperature ^1H NMR spectrum of the tibt compound **8** is quite different. Three signals are observed for the α-, β-, and γ-protons of one pyridine ring, but although the γ-proton triplet of the other ring is clearly resolved, the α- and β-protons appear as two broad signals, each of integration 2 H. Cooling the sample to −55 °C resolves these broad features into four sharp signals, two doublets for the α-protons and two triplets for the β-protons (Figure 4). At this temperature, the ring can no longer rotate, and its configuration relative to the arenethiolate rings causes the two sides of the pyridine ligand to become magnetically inequivalent. It is assumed that this ring is on the more sterically hindered side of the molecule and that the one on the less encumbered side is still rotating rapidly. The room-temperature ^1H NMR spectrum of the less sterically hindered tmbt compound **7** is thus the limiting high-temperature spectrum in which both rings are freely spinning.

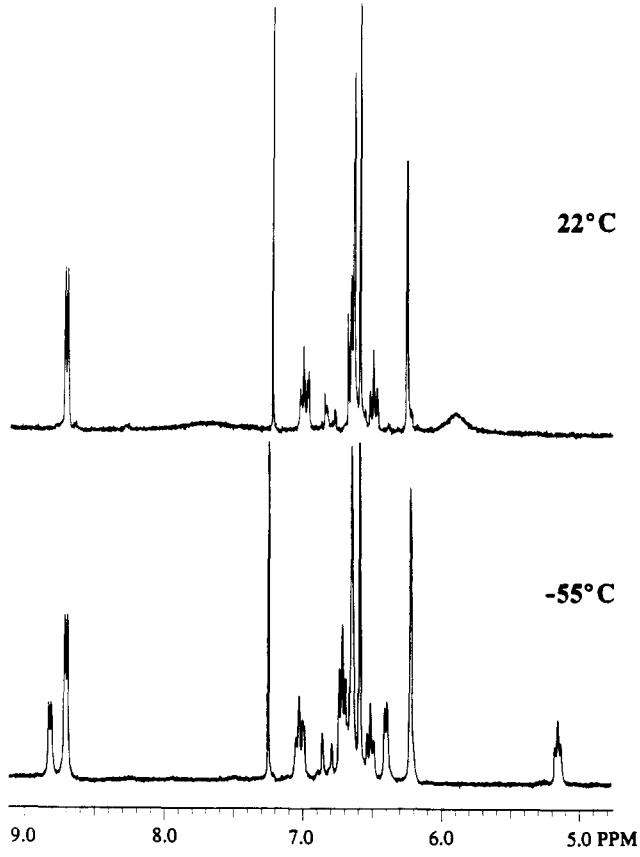

Figure 4. ^1H NMR spectra of **8** at (a) 22 °C and (b) −55 °C.

X-ray Structure Determinations. Suitable X-ray-quality crystals of **1** could not be grown; however, the 2,4,6-triisopropylbenzenethiolate (tibt) analogue **2** provided large prisms, and this compound was subjected to a crystal structure determination. The coordination geometry (Figure 1) of the compound is intermediate between a square pyramid and a trigonal bipyramid according to the criteria of Muetterties et al.[27] This distortion from square-pyramidal geometry is caused by the bending down of the two opposing sulfur atoms from the basal plane and the bending up of the pyridine ligand and the third sulfur atom toward the oxo group. Selected bond distances and angles are presented in Table III. The Tc–O distance is 1.665 (3) Å, which is a typical bond length for the Tc(V) oxo group.[28] In the crystallographically determined structure, all three thiolate ligands are unique. ^1H NMR studies indicate that this conformation of the thiolate rings persists in solution both for this compound and for the tmbt analogue **1**. In each case all three rings are inequivalent and each gives rise to a distinct set of signals. However, the protons on the pyridine ring of each compound appear as only one set of α, β, and γ signals, suggesting that in solution the pyridine ligands are spinning rapidly.

The crystallographic structure determination of the DMSO compound **9** indicates that it shares the same geometry as all other compounds of the series $Tc(SAr)_3L_2$ that have been structurally characterized thus far. The coordination sphere is trigonal bipyramidal (Figure 2) with the thiolate ligands bound in the equatorial plane and the acetonitrile and DMSO groups sitting in the axial positions. There is also the familiar "two-up–one-down" orientation of the arenethiolate rings.[12] DMSO was found to be S-bound and to be on the same side of the equatorial plane as the unique thiolate ring, where steric hindrance is minimized.

(27) $\delta e_1 = 60.5°$; $\delta e_2 = 64.2°$; $\delta e_3 = 31.4°$: Muetterties, E. L.; Guggenberger, L. J. *J. Am. Chem. Soc.* **1974**, *96*, 1748.
(28) Melnik, M.; van Lier, J. E. *Coord. Chem. Rev.* **1987**, *77*, 275.

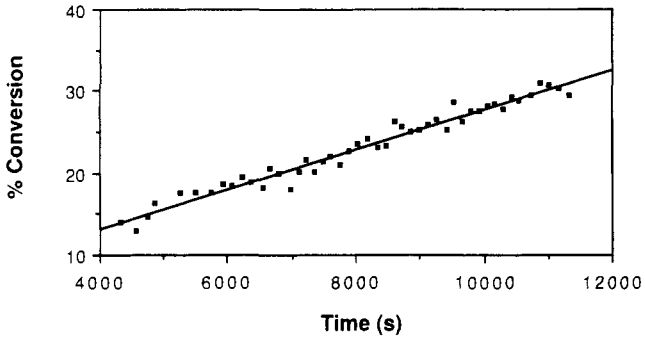

Figure 5. Plot of the rate of the reaction DMSO + PPh_3 → DMS + $OPPh_3$ as catalyzed by **1**. A solution of **1** (4.90 mM), PPh_3 (0.128 M), and DMSO (0.280 M) in MeCN was kept at 22 °C and the ^{31}P NMR spectrum determined every 2 min.

Selected bond lengths and angles are presented in Table VI. The Tc–S bond distances for the thiolate sulfurs (2.261 (3), 2.265 (4), and 2.242 (3) Å) are consistent with those found in the structures of $Tc(tmbt)_3(MeCN)_2$, $Tc(tmbt)_3(MeCN)(CO)$, and $Tc(tmbt)_3(CO)(py)$ (2.248 (3), 2.258 (1), and 2.257 (6) Å, respectively).[12] The Tc–N1 bond length (2.090 (9) Å) is similar to that found in $Tc(tmbt)_3(MeCN)_2$ (2.043 (8) Å).

Oxygen Atom Transfer Reactions. Removal of an oxygen atom from DMSO to yield dimethyl sulfide is a thermodynamically favored process, and DMSO has been shown to transfer oxygen atoms to metal complexes.[2] Compound **6**, $Tc(tmbt)_3(MeCN)_2$, reacts with hot DMSO to produce first a purple compound. Longer reaction times yield an orange compound and, finally, pertechnetate. The orange compound was not isolated, but crystals of the purple material were obtained. This purple compound proved to be unstable in solution and was characterized only by FABMS(+) and by X-ray crystallography. Both of these techniques showed its formulation to be $Tc(tmbt)_3(MeCN)(DMSO)$ (**9**). Instead of being the product of an oxo atom transfer reaction, **9** is the result of axial ligand substitution. This reaction is similar to those described previously for other Tc(III) trithiolate compounds.[12]

Other oxo-transfer reagents were used in further attempts to obtain technetium oxo complexes from **6**. When triethylamine *N*-oxide is allowed to react with compound **6** in refluxing ethanol, a reaction ensues and the color of the solution changes from blue to red-orange; however, as with the DMSO system, no stable products could be isolated from the resulting mixture. In contrast, the analogous reaction of **6** with pyridine *N*-oxide yields $TcO(tmbt)_3(py)$ (**1**) as an orange microcrystalline material. Although all of the above oxo-transfer reagents react with compound **6**, only pyridine *N*-oxide produces a stable Tc(V) oxo compound. Pyridine is a better σ-donating ligand than either Et_3N or DMS, and this may be responsible for its ability to provide a necessary fifth ligand. This being the case, $Tc(tmbt)_3(py)_2$ (**7**), which already contains pyridine ligands, should react with any of the above oxo-transfer reagents to yield $TcO(tmbt)_3(py)$. In fact, compound **7** does react with DMSO, triethylamine *N*-oxide, and pyridine *N*-oxide to give approximately 35% yields of compound **1**. This evidence strongly suggests that, although any one of the above oxo-transfer reagents can effectively oxidize compounds **6** and **7**, DMS and Et_3N are not appropriate ligands to stabilize the resulting Tc(V) oxo product. The low yields observed in all the Tc(III) → Tc(V) reactions are attributed to the further reaction of the Tc(V) product to form $[TcO_4]^-$.

Both Tc(V) oxo complexes **1** and **3** can be reduced by phosphines via oxygen atom abstraction reactions to produce Tc(III) compounds. Although the reaction can be performed with PPh_3, it proceeds much more quickly with the more basic phosphine PEt_3. For the tetrathiolate complex **3**, reduction to Tc(III) is sluggish, requiring a large excess of phosphine and only proceeding at elevated temperatures. However, the neutral compound $TcO(tmbt)_3(py)$ (**1**) is easily reduced at room temperature by a stoichiometric quantity of phosphine. The electrochemical reduction potentials of compounds **1** and **3** show the trend opposite to that expected on the basis of the above observations. Compound **1** is more difficult to reduce electrochemically, despite being more easily reduced by phosphines. Thus, the ease of reduction of compound **1** is likely due to kinetic factors, and displacement of the py ligands by PR_3 may be involved. In support of this, $[TcO(ethanedithiolato)_2]^-$ has been reported not to react with phosphines at all.[7]

The oxidative and reductive oxo-transfer reactions described above can be coupled to provide a catalytic cycle. Addition of a catalytic amount of $TcO(tmbt)_3(py)$ to a solution containing DMSO and PPh_3 causes the transfer of an oxygen atom from DMSO to the phosphine to yield the phosphine oxide and dimethyl sulfide. A number of other compounds can catalyze similar reactions.[2] Most notable is $MoO(LNS_2)$ (LNS_2 = 2,6-bis(2,2-diphenyl-2-mercaptoethyl)pyridine), which was reported by Holm in 1985.[29,30] A common problem with other molybdenum systems is the destruction of the catalyst through the formation of μ-oxo dimers. $MoO(LNS_2)$ circumvents this problem through the use of a chelating ligand that has two phenyl rings which prevent the molybdenum centers from interacting. Technetium can also easily form μ-oxo dimers,[5,31] and the steric bulk of the thiolate ligands probably has a similar role to the LNS_2 ligand. There are two other mechanisms that could destroy the active catalytic species in the technetium system. Prolonged reaction of $TcO(tmbt)_3(py)$ with PEt_3 yields the fully reduced Tc(I) complex $[Tc(PR_3)_6]^+$. However, PPh_3 is too sterically hindered to form $[Tc(PPh_3)_6]^+$. $TcO(tmbt)_3(py)$ is eventually oxidized to $[TcO_4]^-$ by DMSO, but competition of this reaction with reduction by PPh_3 does not appear to be a destructive factor, since the catalyst is still fully active after 500 turnovers as determined by ^{31}P NMR spectroscopy. The rate of catalysis in the system containing compound **1** (Figure 5) and those of **3** and $TcO(SPh)_3(py)$ were also determined by using ^{31}P NMR spectroscopy and found to be 3.0×10^{-2}, 9.8×10^{-3}, and 0.27 turnover/min, respectively. The sterically innocent thiophenol complex catalyzed the same reaction as **1** more rapidly but was more quickly degraded, especially in the presence of a large excess of DMSO, while the more sterically hindered complex **2** proved to be a less active catalyst. This suggests that the rate-limiting step in the oxygen atom transfer cycle is associative.

Acknowledgment. We wish to thank Catherine E. Costello and Cheng-hui Zeng of the NIH Northeast Regional Mass Spectrometry Laboratory for the FAB mass spectra and Michelle Millar for supplying Htmbt and Htibt. N.d.V. is grateful to the American Association of University Women for a Dissertation Fellowship.

Supplementary Material Available: Figures S.A.1 and S.B.1, showing ORTEP diagrams with complete atom-labeling schemes for **1** and **9**, and Tables S.A.I–S.A.V (**1**) and S.B.I–S.B.IV (**9**), listing complete X-ray data, hydrogen atom positional parameters (for **1** only), thermal parameters, intramolecular bond distances, and intramolecular bond angles (19 pages); Tables S.A.VI and S.B.V, listing calculated and observed structure factors (91 pages). Ordering information is given on any current masthead page.

(29) Berg, J. M.; Holm, R. H. *J. Am. Chem. Soc.* **1985**, *107*, 917.
(30) Berg, J. M.; Holm, R. H. *J. Am. Chem. Soc.* **1985**, *107*, 925.
(31) Burgi, H. B.; Anderegg, G.; Blauenstein, P. *Inorg. Chem.* **1981**, *120*, 3829.